A Mononuclear Uranium(IV) Single-Molecule Magnet with a Radical Azobenzene

Maria A. Antunes,[a] Joana T. Coutinho,[a] Isabel C. Santos,[a] Joaquim Marçalo,[a] Laura C. J. Pereira,*[,a] Manuel Almeida,[a] José J. Baldoví,[b] Alejandro Gaita-Ariño*[,b] and Eugenio Coronado.*[,b]

[a] C^{2}TN, Instituto Superior Técnico, Universidade de Lisboa, Estrada Nacional 10, P-2695-066 Bobadela LRS, Portugal

[b] Instituto de Ciencia Molecular, Universitat de València, C/Catedrático José Beltrán 2, E-46980 Paterna, Spain

KEYWORDS Molecular magnetism, uranium, triazacyclononane, single-molecule magnet, radical azobenzene, effective electrostatic model

ABSTRACT: The tetravalent uranium compound with a radical azobenzene ligand [{(SiMe$_2$NPh)$_3$-tacn}U^{IV}(η^2-N$_2$Ph$_2^{\bullet}$)] (**2**) was obtained from a one-electron reduction of azobenzene by the trivalent uranium compound [U^{III}\{(SiMe$_2$NPh)$_3$-tacn\}] (**1**). The new compound **2** was characterized by single crystal X-ray diffraction and ^{1}H NMR spectroscopy. The magnetic properties of this compound as well as those of the precursor **1** were studied by static magnetization and AC-susceptibility measurements. These measurements reveal for the first time in a mononuclear U(IV) compound single-molecule-magnet behavior, while **1** is a rare example of a U(III) compound that does not exhibit slow relaxation of the magnetization at low temperatures. A first approximation to the magnetic behaviors of these compounds was attempted by combining an effective electrostatic model with a phenomenological approach using the full single-ion hamiltonian.

INTRODUCTION

Driven by the new physics and remarkable potential applications in data storage and quantum computing, single-molecule magnets (SMMs) became an important topic of research in the field of molecular magnetism.[1-9] Firstly observed in polynuclear aggregates of paramagnetic transition-metal ions, it was initially believed that high-spin clusters were required to generate such behavior.[1,5] However, in 2003 a seminal work made by Ishikawa and co-workers revealed that bis-phthalocyanine lanthanide(III) compounds containing one single paramagnetic ion, Tb or Dy, exhibited SMM behavior as well.[10] Since then, an increasing number of SMMs based on mononuclear lanthanide compounds[5,11-15] and, more recently, mononuclear actinide[5,16-19] and transition-metal complexes[5,20-22] have been reported. These compounds are generally known as single-ion magnets (SIMs).

In spite of some important advances,[5,6,13,19,23-32] the SMM phenomenon in these mononuclear complexes is far from being well understood. The development of new SIMs with improved magnetic properties is thus still dependent on a more detailed understanding of the parameters underlying slow magnetic relaxation and its mechanism. In this respect it is important to compare related compounds to clearly probe selected effects such as coordination geometry, nature of ligands and crystal field strength, oxidation state of the metal, as well as the effects of magnetic dilution and magnetic exchange coupling. In this context, the study of actinide-based complexes is considered an emerging topic. In fact, due to the properties of the 5f electrons, actinides exhibit stronger spin-orbit coupling interactions, larger magnetic anisotropy and enhanced exchange interactions. Thus, they can be considered as better candidates to provide SIMs than lanthanides, as the J-ground state splitting cause by the ligand field is expected to be higher.[16,19] Although some examples have been reported during the last few years, SIMs based on actinides are still scarce and mainly restricted to U(III) species; aside from a few distinct compounds,[17,18,33,34] most studies have focused on poly(pyrazolyl)borate uranium complexes.[35-43] These studies on wisely selected compounds could put clearly into evidence the effects of axial[34-36,39-41,43] and non-axial ligand environments,[17,18,34,38,42] magnetic dilution,[37] charge of the co-ligand,[38,42] different ligand donor strength in the same trigonal prismatic[41] and tetrahedral[17] coordination geometries, and also the first comparative studies with isostructural lanthanide complexes.[39,41]

The effect of the oxidation state of uranium, which is known to exist in the range +2 to +6, has remained less explored. U(VI) is a diamagnetic ion and on the other extreme molecular U(II) species only very recently have been isolated in the solid state.[44,45] Considering the range +3 to +5, besides the U(III) complexes mentioned above, only one example based on a mononuclear uranium(V) system has been identified[46] and so far no examples of SMMs based on uranium(IV) have been reported. The U(IV) ion, an f^2 system with a $^3H_4$ ground state, is a non-Kramers ion, which generally presents an orbital singlet ground state at low temperatures.[47] Lacking the magnetic bistability of the ground state required for slow magnetic relaxation,[24] U(IV) is thus believed not to be a suitable candidate for generating SIMs,[25] and, in fact, SMM behavior was explicitly reported as absent in some U(IV) compounds.[48-51] However, an appropriate choice of the coordination environment and the presence of a radical may circumvent this constraint. In fact, the possibility of coupling a magnetic ion to an organic radical can have dramatic effects on magnetic relaxation. It has been shown that a radical can slow down quantum

tunneling relaxation pathways.[14] In fact, concerning uranium ions, the presence of a radical ligand in the compound $[U^{III}(Tp^{Me2})_2(bipy^{\bullet})]$ ($bipy^{\bullet}$=radical bipyridine) that induces the appearance of slow magnetic relaxation under zero static magnetic field was recently demonstrated.[42] With lanthanides, a seminal work in this context was reported by J. R. Long and co-workers[52,53] who linked two Dy(III) or two Tb(III) ions via a $[N2]^{3-}$ radical, demonstrating that the system can enhance the exchange coupling between their spins and produce record high blocking temperatures. Nevertheless, while exchange coupling mediated by a radical can block tunnelling when the anisotropy axes of the connected SIMs are parallel, it can enhance tunnelling if they are not.[54] At this point, it is important to remark that the effect of the radical in this kind of complexes is not limited to an enhanced exchange between two metal ions. In a single rare earth ion coupled to a radical ligand dramatic effects are also expected. For example, depending on the symmetry of the system, diagonal or off-diagonal terms will act, blocking or enhancing tunnelling respectively. Additionaly, the presence of an extra electron switches the magnetic system from half- to integer-spin or vice-versa. An illustrative situation is that of a Kramers ion, e.g. Er(III) or U(III), for which tunnelling is strictly forbidden when isolated, but which can be enabled to flip if coupled to a half-integer spin (a radical). In fact, the main effect in this case of the extra electron spin is to switch the parity from Kramers to non-Kramers. Thus, the goal in this work is to apply the same principle to a non-Kramers ion (U(IV)) to produce a Kramers magnetic molecule capable of slow relaxation of the magnetization.

In this paper we report the magnetic properties of a U(IV) complex containing a radical-azobenzene ligand, $[\{(SiMe_2NPh)_3\text{-tacn}\}U^{IV}(\eta^2\text{-}N_2Ph_2^{\bullet})]$ (**2**). This compound is obtained from a one-electron reduction of azobenzene by the previously described trivalent uranium compound $[U^{III}\{(SiMe_2NPh)_3\text{-tacn}\}]$ (**1**).[55] The magnetic properties of **1** were also studied and interestingly it is found to be a rare example of a U^{III} compound which does not exhibits slow relaxation of the magnetization. These results are understood within an effective electrostatic model based on the crystal field theory and the full single-ion hamiltonian.

RESULTS AND DISCUSSION

Synthesis and Structural Characterization. The synthetic strategy used to prepare the compound $[\{(SiMe_2NPh)_3\text{-tacn}\}U^{IV}(\eta^2\text{-}N_2Ph_2^{\bullet})]$ (**2**), known to exist since 2005,[56,57] was based on our work with the trivalent uranium system $[U^{III}\{(SiMe_2NPh)_3\text{-tacn}\}]$ (**1**), which has proven to engage in one-electron reduction of halogenated and chalcogenide substrates to afford U(IV) derivatives,[55,56,58] as well as in two-electron reduction of elemental sulfur leading to the formation of a terminal U(V) persulphide.[58] Thus, the addition of one equivalent of azobenzene to a toluene solution of compound **1** leads to an immediate color change from brown to dark green. The reaction mixture was left stirring for approximately two hours at room temperature, and after appropriate work-up a dark-green powder was isolated in 59% yield. Characterization by ^{1}H NMR spectroscopy and single- crystal X-ray diffraction analysis proved this product to be the uranium(IV) compound with an azobenzene radical anion $[\{(SiMe_2NPh)_3\text{-tacn}\}U^{IV}(\eta^2\text{-}N_2Ph_2)]$ (**2**) (Scheme 1).

Scheme 1. Synthesis of Compound 2.

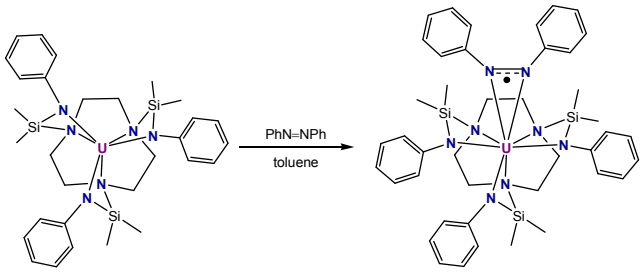

The reduction of azobenzene with formation of a radical anion or even a dianionic ligand has been performed by different lanthanide systems,[59-67] but it was not previously described in uranium chemistry. Actually, the examples reported in the literature concerning the reaction of uranium compounds with azobenzene have always resulted in the reductive cleavage of the N=N bond to form bis(phenylimido) derivatives. These reactions occur by a multi-electron redox process involving the metal center and the ligands in case of U(III) and U(IV)[68-71] or just the metal center in case of U(II).[72-75] The absence of a redox-active ligand in the coordination environment of the U(III) compound (**1**) favors a single-electron reduction process with the concomitant formation of **2** as shown in Scheme 1.

The ^{1}H NMR spectrum of **2**, performed in a benzene-d_6 solution at room temperature, exhibits six broad proton resonances between 22 ppm and -41 ppm for the $\{(SiMe_2NPh)_3\text{-tacn}\}$ ligand (Figure 1). The eighteen protons of the three $SiMe_2$ groups give rise to a single peak at low field, the twelve methylene protons of the aza-macrocyclic ring to two peaks and the fifteen protons of the aromatic rings to three peaks. This pattern suggests that a fluxional process occurs in solution on the NMR time-scale. The resonances accounting for the *ortho*-, *meta*- and *para*- protons of the two phenyl rings of the azobenzene appear as three strongly shifted signals at low field (61.94 ppm) and high field (-146.7 ppm and -189.9 ppm). Chemical shifts of this magnitude are a strong evidence for the presence of a coordinated radical ligand as observed for some lanthanide compounds bearing a $\{N_2Ph_2^{\bullet-}\}$ radical.[60,62]

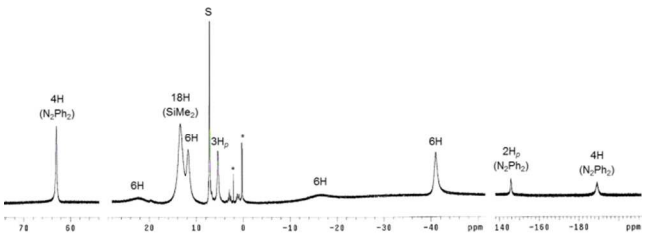

Figure 1. ^{1}H NMR spectrum (300 MHz) of compound **2** in benzene-d_6 at room temperature.

Low-temperature NMR studies were performed on a toluene-d_8 solution of compound **2**. A gradual cooling of the sample resulted in the progressive shifting and broadening of the proton resonances, indicating a slowing of the dynamic process observed at room temperature. At –40 °C all the proton NMR shifts were coalesced in the baseline but by –60 °C the

resonances started to emerge again. At −80 °C, very broad peaks assigned to the {($SiMe_2NPh)_3$-tacn} ligand were observed (Figure 2). At this temperature, the ^{1}H NMR spectrum presents three signals for the $SiMe_2$ protons, six signals for the CH_2 protons of the tacn fragment and three more signals that could be ascribed to the aromatic protons of the NPh groups. The number of resonances for the methyl protons and the macrocyclic amine indicates that in solution the molecule possesses a *pseudo*-C_s symmetry. The existence of only three peaks for the phenylamido groups shows that the fluxional process that makes the protons of these three groups equivalent is still fast at this temperature on the NMR time scale. This fluxional process could be related to changes in the relative position of the phenylamido groups in the coordination sphere around uranium. Considering that the geometry in solution approaches the one found in the solid state (see Figure 3 and discussion below), this process would correspond to the exchange of the nitrogen atoms N4, N5 and N6 between equatorial and capping sites, maintaining the phenyl groups in the symmetry plane. A similar low-temperature spectrum was found for the iodide derivative [{($SiMe_2NPh)_3$-tacn}U^{IV}I].[55]

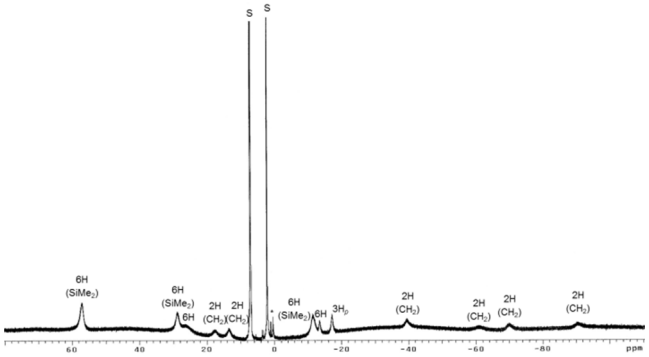

Figure 2. ^{1}H NMR spectrum (300 MHz) of compound **2** in toluene-d_8 at −80 °C.

Compound **2** crystallizes readily as dark green crystals in common solvents such as THF or toluene, however single crystals suitable for X-ray diffraction studies could be obtained only from a benzene-d_6 solution of **2** kept at room temperature. This compound crystallizes in the triclinic P−1 space group, with two crystallographically independent molecules in the asymmetric unit. In each molecule, the uranium atom is octacoordinated by the three nitrogen atoms of the macrocycle, the three nitrogen atoms of the pendant arms and the two nitrogen atoms of the azobenzene (Figure 3(a)), but due to the small bite angle of the azobenzene (N7–U–N8=32.96(9)° in both molecules) it can be considered as if this ligand occupies one single coordination position. The coordinating atoms describe a distorted bicapped trigonal bipyramid around the uranium centers, with the atoms N3/N3A and the midpoint of N7–N8/N7A–N8A bond occupying the axial positions (angles N3–U1–midpoint(N7–N8)= 173.13(9)° and N3A–U2–midpoint(N7A–N8A)= 172.41(8)°), the atoms N1/N1A, N2/N2A, N6/N6A located in the equatorial sites and the atoms N5/N5A and N4/N4A capping two of the triangular faces of the bipyramid (Figure 3(b)). This coordination geometry is quite different from the precursor compound **1** which presented an almost perfect trigonal prismatic coordination geometry (Figure 3(c), (d)).[55]

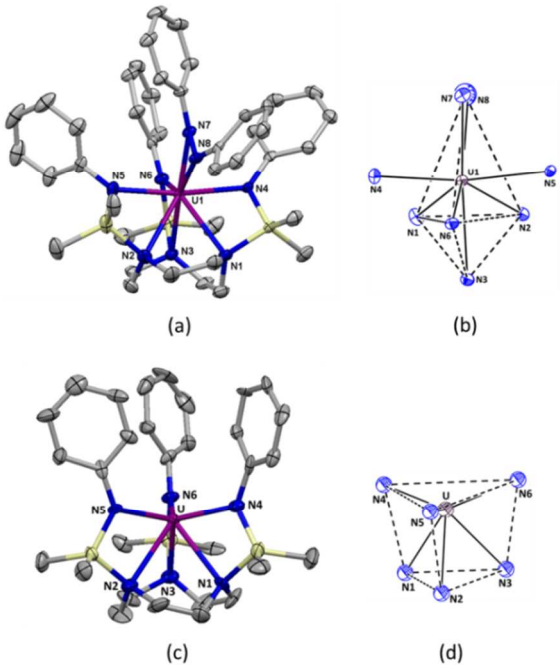

Figure 3. Molecular structures and coordination geometries of (a, b) [{($SiMe_2NPh)_3$-tacn}U^{IV}(η^2-N_2Ph_2)] (**2**) and (c, d) [U^{III}({($SiMe_2NPh)_3$-tacn}] (**1**) (thermal ellipsoids set at a 40% and 20% probability level respectively). Hydrogen atoms, the second independent molecule for **2** and solvent molecule for **1** were omitted for clarity. Bond distances (Å) for **1**: U–N_{amido}=2.326(19)-2.367(15); U–N_{amine}=2.640(18)-2.677(19).[55]

Relevant bond distances and angles and a summary of the crystal data and refinement parameters are given in Table 1 and Table S1, respectively. The two molecules, I and II, feature similar metric parameters but different conformations forming an enantiomeric pair (Figure S1). The bond lengths observed are consistent with the presence of a U(IV) center coordinated to a monoanionic azobenzene ligand, further confirming the evidences shown by the proton NMR spectrum. One clear indication of the radical nature of the azobenzene ligand is the N7–N8/N7A–N8A bond distances (1.353(4) and 1.350(4) Å in molecule I and II), which present a value between the N=N double bond of azobenzene (1.251 Å)[76] and the N–N single bond of hydrazine (1.45 Å in average)[77] comparing well with the ones reported for the related lanthanide complexes [$Cp^*_2Sm(\eta^2$-$N_2Ph_2)$(THF)] (1.32(1) and 1.39(2) Å),[59] [$(Tp^{Me2})_2Sm(\eta^2$-$N_2Ph_2)$] (1.332(12) Å)[60] and [$Ln(\eta^5$-$C_4Me_2R_2P)_2(\eta^2$-$N_2Ph_2)$] (R=^{t}Bu, Ln=Tm; R=SiMe3, Ln=Sm) (1.351(5) and 1.351(4) Å).[63] Furthermore, the U-(η^2-N_2Ph_2) bond distances (2.353(3) and 2.413(3) Å in molecule I and 2.357(2) and 2.400(3) Å in molecule II) are comparable to, although slightly shorter than, the ones found in the complex [{($SiMe_2NPh)_3$-tacn}U^{IV}(η^2-(NHC(Me))$_2$CC≡N}] (2.433(15) and 2.47(2) Å) which bears a bidentante monoanionic N-donor ligand.

The azobenzene is nonsymmetrically bound to the metal center, with distances U–N8/N8A 0.060 and 0.043 Å longer than the U–N7/N7A, as observed in analogous lanthanide complexes.[59,64,65] However, at variance with lanthanide systems, this dissymmetry is not reflected in the bond length between the nitrogen atoms and the *ipso*-carbons of the phenyl rings which present similar values (1.409(4) and 1.408(4) Å

for molecule I and 1.404(4) and 1.409(4) Å for molecule II). The phenyl rings of the azobenzene maintain the same relative orientation as in free cis-azobenzene[76] with slightly less acute dihedral angles (70.37° and 72.15° vs 64.26°), but are significantly more twisted around the N–Ci bonds as attested by the Ci–N–N–Ci torsion angles, which increase from 8° in free azobenzene to 40° in compound **2**. The U–N(amido) and U–N(amine) bond distances range from 2.322(3) to 2.374 Å and 2.625(3) to 2.753(3) Å, respectively, and are in agreement with those reported for the other tetravalent uranium complexes within this family.[55,58,78]

Table 1. Bond distances (Å) and angles (°) for compound 2.

Molecule I		Molecule II	
U1–N1	2.680(3)	U2–N1A	2.726(3)
U1–N2	2.743(3)	U2–N2A	2.753(3)
U1–N3	2.625(3)	U2–N3A	2.645(3)
U1–N4	2.359(2)	U2–N4A	2.374(2)
U1–N5	2.322(3)	U2–N5A	2.334(3)
U1–N6	2.345(3)	U2–N6A	2.337(3)
U1–N7	2.353(3)	U2–N7A	2.357(2)
U1–N8	2.413(3)	U2–N8A	2.400(3)
N7–N8	1.353(4)	N7A–N8	1.350(4)
N7-C31	1.409(4)	N7A-C31A	1.404(4)
N8-C37	1.408(4)	N8A-C37A	1.409(4)
N1–U1–N2	62.23(9)	N1A–U2–N2A	61.71(8)
N1–U1–N3	66.76(9)	N1A–U2–N3A	65.34(8)
N2–U1–N3	68.78(9)	N2A–U2–N3A	67.58(8)
N4–U1–N5	170.57(9)	N4A–U2–N5A	167.04(9)
N4–U1–N6	94.09(9)	N4A–U2–N6A	96.14(9)
N5–U1–N6	88.69(10)	N5A–U2–N6A	92.76(9)
N7–U1–N8	32.96(9)	N7A–U2–N8A	32.96(9)
$(N7–N8)_{midpoint}$–U1–N3	173.13(9)	$(N7A–N8A)_{midpoint}$–U2–N3A	172.41(8)

Magnetic Properties. The temperature dependence of the magnetic susceptibility of complexes **1** and **2** was measured in the range 3 to 300 K under a static field of 1000 Oe (Figure 4), revealing a paramagnetic behavior for both compounds. The χT product at room temperature for **1**, 0.94 emu·K·mol^{-1}, is lower than the reported value for the $5f^3$ U^{3+} free-ion but within the observed values for U(III) compounds.[79] For compound **2** the χT product drops monotonically from 1.32 emu·K·mol^{-1} at 300 K to 0.68 emu·K·mol^{-1} at 3 K. The χT value at 300 K is lower than the expected free-ion value for the $5f^2$ U(IV), 1.60 emu·K·mol^{-1}, but slightly higher than the average values (0.78-1.19 emu·K·mol^{-1}) found in most of U(IV) compounds.[79,80] This is certainly due to the additional contribution of the extra spin from the radical azobenzene which seems to be ferromagnetically coupled to the U(IV) center. A similar increase of the magnetic moment due to the radical ligand contribution was already observed in the U(III) complex $[U(Tp^{Me2})_2(bipy\bullet)]$[42] although in this case the extra magnetic moment of the bipyridine radical ligand was coupled antiferromagnetically to the central ion. At 3 K a magnetization of 2.33 μ_B was measured. This significant high value at low temperatures is not unusual, being found in charge-separated uranium(IV) species with centered radical ligands.[81,82] High magnetic moment values at low temperatures were also found in uranium(IV) compounds presenting a trigonal bipyramidal geometry of $[Li(DME)_3][U(CH_2SiMe_3)_5]$ and $[Li(THF)_4][U(CH2^tBu)5]$ leading to changes in the crystal field splitting patterns.[83]

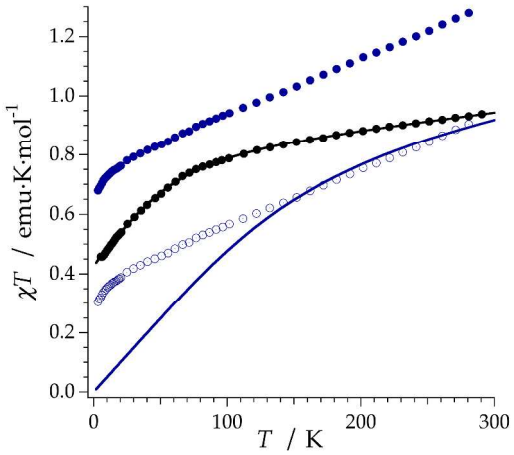

Figure 4. (a) Experimental (symbols) and calculated (solid line) temperature-dependence of the magnetic susceptibility as χT product for compound **1** (black) and **2** (blue), from 2 to 300 K using the CONDON package (see text). The behavior of **2** without the radical contribution (assumed to be equal to 0.375 emu·K·mol^{-1}) is reported as open circles.

The magnetic field dependence of magnetization of **1** (Figure S2) and **2** (Figure S3) was measured at several temperatures under fields up to 5 T using a SQUID magnetometer at temperatures down to 0.3 K (sweep rate 0f 20 Oes^{-1}) and under fields up to 10 T using a MagLab 2000 system (Oxford Instruments) at temperatures down to 1.7 K (sweep rate of 90 Oes^{-1}). For compound **1** no hysteresis was observed down to 1.7 K even with a sweeping rate of 90 Oe s^{-1}.

For compound **2,** as shown in the inset of Figure S3, an opening of the hysteresis curves could be clearly observed at 1.7 K, with a butterfly shape emerging although without zero field coercivity, as typically observed in other mononuclear U(III)[37,40] and U(V)[46] complexes with SMM behavior. This hysteresis becomes more evidenced at even lower temperatures (Figure 5). The absence of coercivity is probably due to an efficient quantum tunneling of the magnetization at zero field caused by low-symmetry components of the crystal field. Despite this, at 0.33 K it is observable the onset of a plateau at half value of the magnetization between 0.15 and 0.5 T. A more clear evidence for this intermediate magnetization state should wait for a complementary study of magnetization under different magnetic field sweeping rates and at even lower temperatures.

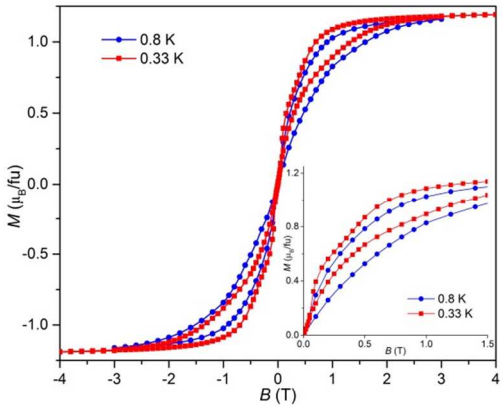

Figure 5. Field dependence of the magnetization at low temperatures at 0.8 and 0.33 K for **2**. The inset shows the curve details up to 1.5 T

An effective charge electrostatic model can be used to understand the magnetic behavior of both compounds. In a first step the Radial Effective Charge (REC) model[84] was applied to the idealized structure (C_{3v}) of **1**, introducing the coordinates of the donor atoms in the SIMPRE computational package.[85] As these ligands have not been parameterized before, for an initial guess of crystal field parameters (CFPs), the effective distances were calculated using the following formula for D_r:

$$D_r \approx \left(\frac{N_L}{V_M}\right) \cdot \frac{1}{E_M(E_L - E_M)}$$

where N_L is the coordination number of the complex, V_M is the valence of the metal, and E_M and E_L are the Pauling electronegativities of the metal and the donor atom, respectively. Such relation was obtained by fitting the phenomenological crystal field parameters of the families $CsNaYCl_6:Ln^{3+}$ and $CsNaYF_6:Ln^{3+}$, $LiYF_4:Ln^{3+}$ and $LaCl_3:Ln^{3+}$ using the crystal structures and the REC model.[86] Subsequently, the effective charge of the donor atoms was calculated assuming a similar relation Z_{eff}/D_r to the observed between the REC parameters of different nitrogen-coordinated compounds studied by this model.[25,84,87]

This strategy allowed us to obtain a set of starting CFPs for fitting the temperature-dependent susceptibility of **1** using a full model approach. As Kögerler *et al.* recently pointed out, the challenge in modeling actinide complexes arrives from the fact that interelectronic repulsion ($\approx 10^4$ cm^{-1}), spin-orbit coupling ($\approx 10^3$ cm^{-1}) and ligand field potential ($\approx 10^3$ cm^{-1}) are roughly of the same order of magnitude.[88] Thus, we introduced this initial trial of calculated CFPs in the package CONDON,[89] which is suitable to model these systems due to the numerical approach that takes into account all the energetic effects of the free ion and the ligand field. The temperature-dependent magnetic susceptibility data was fitted using the full single-ion Hamiltonian approach with the assumptions: ζ_{5f} = 1516 cm^{-1}, F^2 = 36130 cm^{-1}, F^4 = 26000 cm^{-1}, F^6 = 21000 cm^{-1},[90] and a C_{3v} ligand field symmetry. This symmetry approximation implies that the only non-vanishing ligand field parameters are B_{20}, B_{40}, B_{43}, B_{60}, B_{63} and B_{66}. The least-squares fit (SQ = 0.31%) yields B_{20} = -4900 cm^{-1}, B_{40} = 1788 cm^{-1}, B_{43} = 2144 cm^{-1}, B_{60} = 4363 cm^{-1}, B_{63} = -7055 cm^{-1} and B_{66} = 8166 cm^{-1}.

The overall ligand field splitting of the ground multiplet J = 9/2 is about 1800 cm^{-1}. This highest state of the ground multiplet is separated from the lowest state of the following first excited multiplet J = 11/2 only by 1750 cm^{-1}, which is located at 3550 cm^{-1}. This evidences the need of using a full approach instead of an effective one (assuming Russell-Saunders coupling) for a proper description of the system. All 182 doublets covered by the application of the full basis span an energy interval of ca. 65970 cm^{-1}. The ground doublet is mainly composed of M_J = 42% |±5/2> + 36% |±1/2> + 22% |±7/2> states. The presence of an important contribution of ±1/2 in the ground doublet explains the inability of **1** to display SMM behavior. This is also denoted by the crystallographic structure of the compound, where the three nitrogen atoms of the $SiMe_2NPh$ group are placed at 77° in average from the polar coordinate in θ, i.e. complex **1** illustrates a situation where the electron density is distributed near the plane xy. Since U(III) is an oblate ion with the f-electron density equatorially distributed, the repulsive contacts between ligand and *f*-electron charge cloud do not favor the stabilization of a high M_J value in the ground doublet. Thus, contrary to the conclusions of ref. 33, compound **1** evidences that specific symmetries or ligand surroundings may have crucial effects in the magnetic properties of uranium complexes.

Regarding the simulation of the magnetic properties, the fitted χT product and the predicted magnetizations using the full single-ion hamiltonian in the CONDON computational package (Figure 4, solid black line) are in excellent agreement with experimental data. The magnetization predicted by this model at 2 K (Figure S3) is essentially exact at low field/temperature ratios (H/T < 1 T/K). There are some deviations at higher fields or lower temperatures, where the predicted magnetization rises above the experimental data which can be related to small dipolar interactions between the U(III) centers becoming relevant at lower temperatures.

In a second step, the REC model was used again to obtain an estimation of D_r and Z_i of the groups tacn (D_r = 1.52 Å and Z_i = 0.04) and $SiMe_2NPh$ (D_r = 0.18 Å and Z_i = 2.64) by a direct fitting of the phenomenological CFPs determined by CONDON using the idealized structure. These results, combined with an analogous study with pyrazolyl ligands in [$U^{III}Tp_3$] (D_r = 1.48 Å and Z_i = 0.023),[25] allowed us to obtain an estimation of the CFPs of compound **2**. For that, we introduced the crystal structure of compound **2** in the SIMPRE package, corrected by the determined D_r values, just to obtain a set of CFPs.

Finally, we moved again to CONDON in order to calculate the spectroscopic and magnetic properties arising from these CFPs after diagonalizing the full single-ion hamiltonian. It is important to note that in this case the presence of a radical and the lack of symmetry elements in the coordination environment impede the usual strategy of a direct fitting of the data. This is especially due to the overparametrization nightmare that arises from the geometry of the system. In this sense, combining first-principles calculations with model hamiltonians in order to determine the exchange interaction between the *f* and the *p* spins would be a reasonable mid-term goal for the study of this system. Nevertheless, the predicted CFPs using the REC model and the subsequent diagonalization employing the full single-ion hamiltonian allows a reasonable prediction of the χT curve (Figure 4, solid blue line).

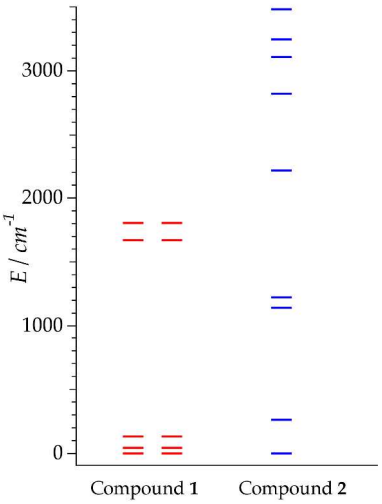

Figure 6. Energy level scheme of the ground multiplet for the magnetic metal ion in compounds **1** and **2**.

The agreement at high temperatures is remarkable, considering that the whole theoretical analysis up to this point has been done in the absence of any experimental magnetic data for **2** and is thus a structurally-guided effective charge electrostatic prediction. Assuming that this theoretical calculation is essentially correct for the U(IV) ion, the observed deviation from experimental data, which starts below 150 K, can be understood as a ferromagnetic exchange coupling between the spin of the radical, and the moment of the U(IV) ion. This coupling is not unexpected since the sp^2 and the *5f* orbitals of the radical and uranium ion present a strong interaction. In this respect it is worth recalling that actinide *5f* orbitals are considerably more diffuse than lanthanide *4f* orbitals making strong interaction. The analysis of the orientations of the *f* and *p* orbitals that would be necessary to fully explain this postulated ferromagnetic exchange is well beyond the scope of this work. The end result is that the experimental χT product at the low temperature limit is of the order of 0.7 emu.K.mol^{-1}, while the calculated value for the U(IV) ion in the absence of the radical would be practically zero. The calculations were performed using the full single-ion Hamiltonian approach with the default assumptions for U(IV): ζ_{5f} = 1926 cm^{-1}, F^2 = 76557 cm^{-1}, F^4 = 50078 cm^{-1}, F^6 = 36429 cm^{-1}, and C_s ligand field. The energy level scheme of the ground multiplet for U(IV) in compound **2** is reported in Figure 6. According to our calculations, the ground state shows an important contribution of M_J = ±4 (74%) but also there is a presence of M_J= 0 (17%) in the easy axis. Thus, the interaction with the radical seems to play a key role in the slow relaxation of the magnetization in complex **2**, while the mere presence of this axial ligand would not be enough. In other words, an equivalent ligand field produced by a diamagnetic but otherwise similar coordination sphere would produce a magnetic behavior similar to that observed in **1**.

Regarding the radical contribution, the main effect of the extra electron spin is to switch the parity from non-Kramers to Kramers. A moderate magnetic exchange suffices to alter the quantum-mechanical character of the ground state doublet. Thus, from a tunnel-splitted doublet that is mainly a mixture of M_J=+4, M_J=-4 and M_J=0 one expects to obtain two doublets that are dominated by M_J=±9/2 and M_J=±7/2, respectively. Solving a complete model considering the U(IV) ion, including its excited states, together with the radical, was impractical at this point. Nevertheless, a toy model consisting of an anisotropic effective S=1 (non-Kramers) exchange-coupled with a S=1/2 suffices to evidence this (details in the SI). Seen from the point of view of the radical, the coupling to the anisotropic magnetic momentum produces an extremely anisotropic radical. Indeed, it has not been possible to observe an EPR signal of **2** in a commercial setup, and this is attributed to an intrinsically broadness of the signal. Experiments concerning this point are ongoing with specialized EPR equipment.

Further information on the magnetization dynamics was obtained by AC susceptibility measurements at low temperatures, 1.6-10 K, with an AC field of 5 Oe in the frequency range 10 Hz – 10 kHz, and under several static magnetic DC fields. For compound **1** no evidence for slow magnetic relaxation was observed with both the in-phase, χ′, and out-of-phase, χ′′, components of susceptibility being frequency independent, even under different static magnetic fields. This is not the situation of complex **2** which although at zero field presents χ′ and χ′′ components frequency independent (Figure S5) it starts to show a strong frequency dependence upon the application of a small static (DC) field. By studying the AC susceptibility at different applied static magnetic fields the slowest relaxation time was observed close to 1000 Oe (Figure S6). With temperature variation a well resolved local maximum appears in χ′′ shifting to higher temperatures as the frequency increases, as shown in Figure 7(b). Above 1000 Oe the magnetic field only slightly enhances the frequency and temperature dependence of the peaks, with χ′ showing broad maxima (Figure 7(c)), and the maxima of χ′′ becoming better resolved for low frequencies (Figure 7(d)) with no significant increase in the magnitude of the peaks (see also Figure S6 in the Supporting Information).

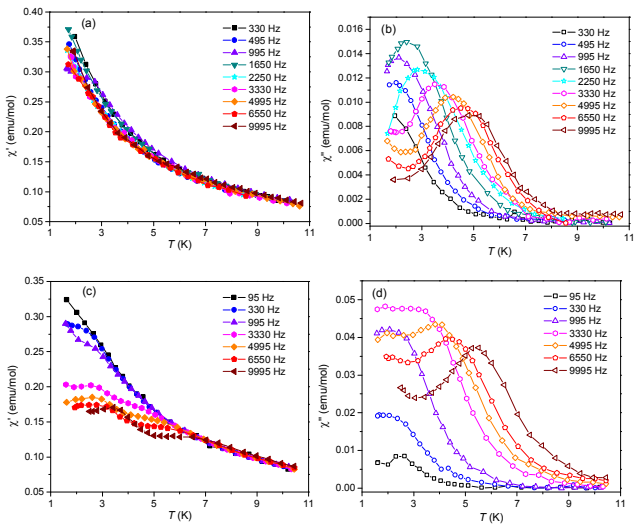

Figure 7. In-phase and out-of-phase components of AC susceptibility at different frequencies from 1.7 to 10K for **2** at H_{AC}=5 Oe and H_{DC} =1000 Oe ((a), (b)), and 2500 Oe ((c), (d)).

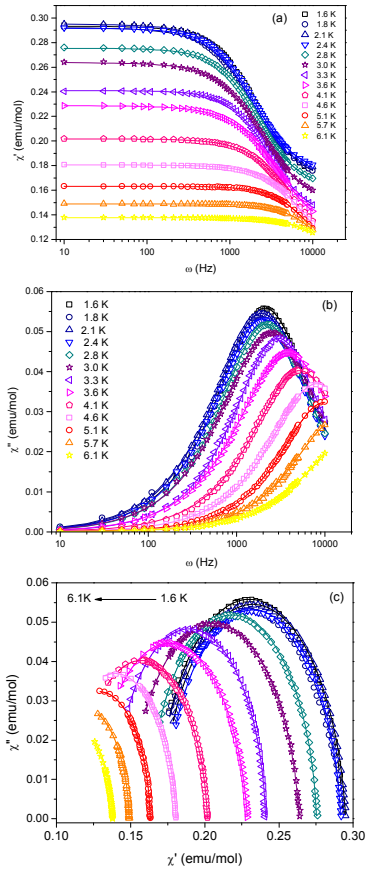

Figure 8. (a) In-phase and (b) out-of-phase components of AC susceptibility at different frequencies in the 1.7 to 10K temperature range for **2** at H_{AC}=5 Oe and H_{DC} =2500 Oe. (c) Cole-Cole plots with best Debye model fits.

At fixed temperatures, between 1.6 and 6 K, the frequency dependence of the AC susceptibility also shows slow magnetic relaxation under applied static DC fields, (Figure 8(a) and (b)) and Supporting Information Figures S7, S8 and S9) clearly denoting SMM behavior with reduction of the Quantum Tunneling of Magnetization (QTM) through spin-reversal barrier via degenerate $\pm M_J$ levels. Using the $\chi(\omega)$ data for three different values of static fields, Cole–Cole diagrams in the temperature range 1.6–6 K were obtained exhibiting semi-circular shapes (Figure 8(c) and Figures S7-S9) fitted using the generalized Debye model,[91] affording α values less than 0.1 (see Tables S2-S4), which support the existence of a single relaxation process.

Magnetization relaxation times could also be extracted considering that compound **2** is relaxing via a thermally activated Orbach process. As seen in Figure 9(a) the Arrhenius law fits, essayed using the equation, $\tau = \tau_0 \exp(U/k_BT)$ where U is the effective energy barrier and k_B is the Boltzmann constant, yielded barriers of U = 14.1, 16.9 and 17.6 K at 1000, 2000, and 2500 Oe, respectively, of the same order of magnitude as those observed for mononuclear U(III) complexes.[17,19,38,40,42] Below 3.5 K it is approached a temperature independent regime of the relaxation time that is similar for all different static fields. This linear relationship of ln(1/τ) with 1/T, indicative of an Orbach process, does not cover the whole range of temperature-dependent data. Thus, in order to find some other contributions to the relaxation pathway a Raman process was then fitted to these experimental data assuming $1/\sqrt[9]{\tau} = a+b\cdot T$, i.e. a linear slope in $1/\sqrt[9]{\tau}$ *vs* *T*. These results can be seen in Figure 9(b) where coefficients a = 2.2, 2.22, and 2.17 and b = 0.21, 0.23, and 0.25 were obtained for static fields of 1000, 2000 and 2500 Oe, respectively. By comparison to the Orbach process these fits clearly show that Raman process covers a wider range of temperatures, in particular at 1000 Oe where only below 2 K an independent temperature regime due to quantum tunnelling effects dominates.

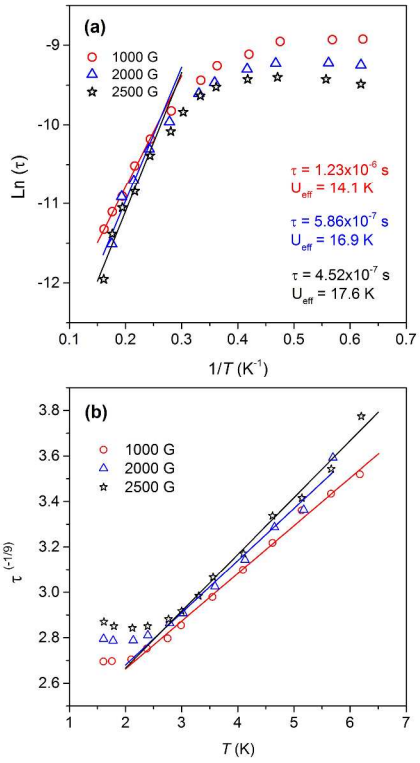

Figure 9. (a) Plot of ln(τ) vs. T^{-1} with fittings to the Arrhenius law. (b) Plot of 9th root of the relaxation frequency *vs* temperature with fittings assuming a Raman process. H_{DC} = 1000 Oe (red), H_{DC} = 2000 Oe (blue), and H_{DC} = 2500 Oe (black); H_{AC} = 5 Oe.

EXPERIMENTAL SECTION

General Considerations. All manipulations were carried out under a nitrogen atmosphere in a glovebox or using standard Schlenk and vacuum-line techniques. Toluene and n-hexane were pre-dried using 4 Å molecular sieves, freshly distilled from sodium/benzophenone under nitrogen atmosphere and degassed with freeze pump-thaw cycles. Benzene-d_6 and toluene-d_8 were vacuum distilled from sodium/benzophenone and stored in PTFE-valve-glass ampoules under nitrogen. Azobenzene was purchased from Aldrich and dried under vacuum prior to use. [U{$(SiMe_2NPh)_3$-tacn}] (**1**) was prepared according to a previously reported procedure.[55] ^{1}H NMR spectra were recorded at 296 K on Varian INOVA-300 and Bruker AvanceII 300 spectrometers. Chemical shifts were referenced to resonances of the residual protonated solvents relative to tetramethylsilane (benzene-d_6, δ 7.16 ppm; toluene-d_8, δ 2.09 ppm). CHN elemental analyses were performed in-house using a EA1110 CE Instruments automatic analyzer.

Synthesis and Characterization of Compound 2. A toluene solution of azobenzene (33 mg, 0.18 mmol) was added dropwise, at room temperature, to a solution of [U{(SiMe$_2$NPh)$_3$-tacn}] (**1**) (145 mg, 0.18 mmol) in the same solvent. A color change from dark brown to dark green was immediately observed. The reaction mixture was left stirring for two hours. After this time, the solvent was evaporated under reduced pressure yielding a dark green solid, which was washed with n-hexane and vacuum dried (Yield: 106 mg, 59%). Elemental analysis for $C_{42}H_{55}N_8Si_3U$: Calculated – C 50.74, H 5.58, N 11.27; Found - C 49.79, H 5.91, N 11.15. 1H NMR (C_6D_6, 300.1 MHz, 296 K): δ (ppm) 61.94 (s, 4H, N_2Ph_2), 22 (vbr, 6H), 13.23 (s, 18H, $SiMe_2$), 11.67 (s, 6H), 5.36 (s, 3H, H_p-NPh), –17 (vbr, 6H), -40.81 (s, 6H), –146.7 (s, 2H, Hp-N_2Ph_2), –189.9 (s, 4H, N_2Ph_2). 1H NMR (toluene-d_8, 300.1 MHz, 193 K): δ (ppm) 57.08 (s, 6H, $SiMe_2$), 28.75 (s, 6H, $SiMe_2$), 26 (vbr, 6H, NPh), 18.1 (br, 2H, CH_2), 13.1 (br, 2H, CH_2), –11.27 (s, 6H, $SiMe_2$), –13.18 (s, 6H, NPh), –17.24 (s, 3H, Hp-NPh), –39.69 (br, 2H, CH_2), –60 (vbr, 2H, CH_2), –69.8 (br, 2H, CH_2), –91 (vbr, 2H, CH_2). No resonances for N_2Ph_2 were observed at this temperature.

Single-Crystal X-ray Diffraction Analysis. A single crystal of compound **2** was selected and coated with FOMBLIN Y60 LVAC 25/6 oil (Aldrich) in a glove box and rapidly mounted on a Bruker AXS-KAPPA APEX II CCD area-detector diffractometer using graphite-monochromated Mo Kα radiation (λ = 0.71073 Å). Cell parameters were retrieved using Bruker SMART S5 software and refined using Bruker SAINT on all observed reflections.[92] Absorption corrections were applied using SADABS.[93] The structure was solved by direct methods using program SIR97[94] and refined by full-matrix least squares refinement on F2 using program SHELXL-97,[95] both included in the package of software programs WINGX.[96] All non-hydrogen atoms were refined with anisotropic thermal motion parameters. All hydrogen atoms were inserted at calculated positions based on the geometries of their attached carbon atoms. The illustration of the molecular structure was made with Mercury 3.3.[97] CCDC reference number: 1054616.

Magnetic Properties. To study the magnetic properties of [U{(SiMe$_2$NPh)$_3$-tacn}] (**1**) and [{(SiMe$_2$NPh)$_3$-tacn}U^{IV}(η^2-N_2Ph_2)] (**2**) two different batches were measured as crystalline powder imbedded in *n*-hexane with identical results within experimental uncertainty. Due to their high air sensitivity, the samples were sealed under vacuum inside a quartz tube. Magnetization was measured using a 6.5 T S700X SQUID magnetometer (Cryogenic Ltd.) in the temperature range 2 – 300 K at several magnetic fields and with a ^{3}He insert for measurements down to 0.3 K. Additional field dependent magnetization up to 10 T (and 10 T at 1.7 K) and AC susceptibility measurements were taken using a MagLab 2000 system (Oxford Inst.) at temperatures down to 1.7 K. The paramagnetic data was obtained after the correction for the core diamagnetism estimated from Pascal's constants, as χ_D=-397.3x10^{-6} emu/mol and χ_D=-501.3x10^{-6} emu/mol for compounds **1** and **2**, respectively.

CONCLUSION

In this work we have prepared and characterized a new mononuclear U(IV) complex with a radical azobenzene ligand [{(SiMe$_2$NPh)$_3$-tacn}U^{IV}(η^2-N_2Ph_2)] (**2**) which is the first example of a compound generated by one-electron reduction of azobenzene performed by a uranium species, [{(SiMe$_2$NPh)$_3$-tacn}U^{III}] (**1**). At variance with several trivalent uranium compounds recently studied, the magnetic properties of **1** do not present any sign of slow relaxation of the magnetization at low temperatures, evidencing the crucial role of the coordination environment. In contrast, compound **2** presents at low temperatures a clear indication of slow relaxation of the magnetization under applied static DC fields in the range 1-2.5 kOe, and a large hysteresis in the magnetization curves, being the first uranium(IV) compound with SMM behavior. The relaxation barrier associated with the thermally activated regime of the relaxation, 17.6 K for 2500 Oe, is of the same order of magnitude as those observed for mononuclear U(III) complexes with SMM behavior. This unprecedented behavior among uranium(IV) seems to result from the interaction of the metal ion with the paramagnetic ligand, which switches the parity from non-Kramers to Kramers. This may provide a new strategy to design SIMs in non-Kramers ions. When considering the use of this strategy to extend relaxation times in rare earth complexes, it is important to consider that tunnelling can only be blocked for temperatures much smaller than the coupling energy. Therefore, in order to achieve a significant success in enhancing the blocking temperature, the exchange coupling to and via the radical must be significant, which is exceptional for lanthanides but more common in actinoids.

ASSOCIATED CONTENT

Supporting Information. Crystallographic data for compound **2**, magnetic data and details of the toy model for the radical contribution. This material is available free of charge via the Internet at http://pubs.acs.org.

AUTHOR INFORMATION

Corresponding Authors

* Email: lpereira@ctn.ist.utl.pt
* Email: alejandro.gaita@uv.es
* Email: eugenio.coronado@uv.es

Author Contributions

The manuscript was written through contributions of all authors. All authors have given approval to the final version of the manuscript.

Funding Sources

EU, FCT (Portugal), Spanish MINECO and Generalitat Valenciana (Spain).

ACKNOWLEDGMENT

The experimental support of Joaquim Branco is gratefully acknowledged. J.T.C. and M.A.A. thank FCT (Portugal) for doctoral and post-doctoral grants (SFRH/BD/84628/2012 and SFRH/BPD/74194/2010). This work was partially supported by FCT (Portugal) under contracts PTDC/QEQ-SUP/1413/2012 and RECI/QEQ-QIN/0189/2012, the EU (ERC Advanced Grant SPINMOL and ERC Consolidator Grant DECRESIM), the Spanish MINECO (grant MAT2011-22785), and the Generalitat Valenciana (Prometeo and ISIC Programmes of excellence). A.G.-A. acknowledges funding by the MINECO (Ramón y Cajal contract). J.J.B. thanks the Spanish MINECO for an FPU predoctoral grant.

REFERENCES

(1) Gatteschi, D.; Sessoli, R. *Ang. Chem., Int. Ed.* **2003**, *42*, 268-297.

(2) Dei, A.; Gatteschi, D. *Ang. Chem., Int. Ed.* **2011**, *50*, 11852-11858.
(3) Mannini, M.; Pineider, F.; Danieli, C.; Totti, F.; Sorace, L.; Sainctavit, P.; Arrio, M. A.; Otero, E.; Joly, L.; Cezar, J. C.; Cornia, A.; Sessoli, R. *Nature* **2010**, *468*, 417-421.
(4) Gatteschi, D.; Sessoli, R.; Villain, J. *Molecular Nanomagnets*; Oxford University Press, 2006.
(5) Layfield, R. A. *Organometallics* **2014**, *33*, 1084-1099.
(6) Pedersen, K. S.; Bendix, J.; Clerac, R. *Chem. Commun.* **2014**, *50*, 4396-4415.
(7) Clemente-León, M.; Coronado, E.; Gómez-García, C. J.; López-Jordà, M.; Camón, A.; Repollés, A.; Luis, F. *Chem. – Eur. J.* **2014**, *20*, 1669-1676.
(8) Luzon, J.; Sessoli, R. *Dalton Trans.* **2012**, *41*, 13556-13567.
(9) Sorace, L.; Benelli, C.; Gatteschi, D. *Chem. Soc. Rev.* **2011**, *40*, 3092-3104.
(10) Ishikawa, N.; Sugita, M.; Ishikawa, T.; Koshihara, S.-y.; Kaizu, Y. *J. Am. Chem. Soc.* **2003**, *125*, 8694-8695.
(11) Feltham, H. L. C.; Brooker, S. *Coord. Chem. Rev.* **2014**, *276*, 1-33.
(12) Zhang, P.; Guo, Y.-N.; Tang, J. *Coord. Chem. Rev.* **2013**, *257*, 1728-1763.
(13) Woodruff, D. N.; Winpenny, R. E. P.; Layfield, R. A. *Chem. Rev.* **2013**, *113*, 5110-5148.
(14) Demir, S.; Jeon, I.-R.; Long, J. R.; Harris, T. D. *Coord. Chem. Rev.* **2015**, *289-290*, 149-176.
(15) AlDamen, M. A.; Clemente-Juan, J. M.; Coronado, E.; Martí-Gastaldo, C.; Gaita-Ariño, A. *J. Am. Chem. Soc.* **2008**, *130*, 8874-8875.
(16) Magnani, N. *Int. J. Quantum Chem.* **2014**, *114*, 755-759.
(17) Pereira, L. C. J.; Camp, C.; Coutinho, J. T.; Chatelain, L.; Maldivi, P.; Almeida, M.; Mazzanti, M. *Inorg. Chem.* **2014**, *53*, 11809-11811.
(18) Goodwin, C. A. P.; Tuna, F.; McInnes, E. J. L.; Liddle, S. T.; McMaster, J.; Vitorica-Yrezabal, I. J.; Mills, D. P. *Chem. – Eur. J.* **2014**, *20*, 14579-14583.
(19) Meihaus, K. R.; Long, J. R. *Dalton Trans.* **2015**, *44*, 2517-2528.
(20) Saber, M. R.; Dunbar, K. R. *Chem. Commun.* **2014**, *50*, 12266-12269.
(21) Samuel, P. P.; Mondal, K. C.; Amin Sk, N.; Roesky, H. W.; Carl, E.; Neufeld, R.; Stalke, D.; Demeshko, S.; Meyer, F.; Ungur, L.; Chibotaru, L. F.; Christian, J.; Ramachandran, V.; van Tol, J.; Dalal, N. S. *J. Am. Chem. Soc.* **2014**, *136*, 11964-11971.
(22) Ruamps, R.; Batchelor, L. J.; Guillot, R.; Zakhia, G.; Barra, A.-L.; Wernsdorfer, W.; Guihery, N.; Mallah, T. *Chem. Sci.* **2014**, *5*, 3418-3424.
(23) Neese, F.; Pantazis, D. A. *Faraday Discuss.* **2011**, *148*, 229-238.
(24) Rinehart, J. D.; Long, J. R. *Chem. Sci.* **2011**, *2*, 2078-2085.
(25) Baldovi, J. J.; Cardona-Serra, S.; Clemente-Juan, J. M.; Coronado, E.; Gaita-Arino, A. *Chem. Sci.* **2013**, *4*, 938-946.
(26) Baldoví, J. J.; Cardona-Serra, S.; Clemente-Juan, J. M.; Coronado, E.; Gaita-Ariño, A.; Palii, A. *Inorg. Chem.* **2012**, *51*, 12565-12574.
(27) Blagg, R. J.; Ungur, L.; Tuna, F.; Speak, J.; Comar, P.; Collison, D.; Wernsdorfer, W.; McInnes, E. J. L.; Chibotaru, L. F.; Winpenny, R. E. P. *Nat. Chem.* **2013**, *5*, 673-678.
(28) Habib, F.; Murugesu, M. *Chem. Soc. Rev.* **2013**, *42*, 3278-3288.
(29) Demir, S.; Zadrozny, J. M.; Long, J. R. *Chem. – Eur. J.* **2014**, *20*, 9524-9529.
(30) Lucaccini, E.; Sorace, L.; Perfetti, M.; Costes, J.-P.; Sessoli, R. *Chem. Commun.* **2014**, *50*, 1648-1651.
(31) Zhang, P.; Zhang, L.; Tang, J. *Dalton Trans.* **2015**, *44*, 3923-3929.
(32) Atanasov, M.; Aravena, D.; Suturina, E.; Bill, E.; Maganas, D.; Neese, F. *Coord. Chem. Rev.* **2015**, *289-290*, 177-214.
(33) Mills, D. P.; Moro, F.; McMaster, J.; van Slageren, J.; Lewis, W.; Blake, A. J.; Liddle, S. T. *Nat. Chem.* **2011**, *3*, 454-460.
(34) Moro, F.; Mills, D. P.; Liddle, S. T.; van Slageren, J. *Angew. Chem., Int. Ed.* **2013**, *52*, 3430-3433.
(35) Rinehart, J. D.; Long, J. R. *J. Am. Chem. Soc.* **2009**, *131*, 12558-12559.
(36) Rinehart, J. D.; Meihaus, K. R.; Long, J. R. *J. Am. Chem. Soc.* **2010**, *132*, 7572-7573.
(37) Meihaus, K. R.; Rinehart, J. D.; Long, J. R. *Inorg. Chem.* **2011**, *50*, 8484-8489.
(38) Antunes, M. A.; Pereira, L. C. J.; Santos, I. C.; Mazzanti, M.; Marcalo, J.; Almeida, M. *Inorg. Chem.* **2011**, *50*, 9915-9917.
(39) Rinehart, J. D.; Long, J. R. *Dalton Trans.* **2012**, *41*, 13572-13574.
(40) Coutinho, J. T.; Antunes, M. A.; Pereira, L. C. J.; Bolvin, H.; Marcalo, J.; Mazzanti, M.; Almeida, M. *Dalton Trans.* **2012**, *41*, 13568-13571.
(41) Meihaus, K. R.; Minasian, S. G.; Lukens, W. W.; Kozimor, S. A.; Shuh, D. K.; Tyliszczak, T.; Long, J. R. *J. Am. Chem. Soc.* **2014**, *136*, 6056-6068.
(42) Coutinho, J. T.; Antunes, M. A.; Pereira, L. C. J.; Marcalo, J.; Almeida, M. *Chem. Commun.* **2014**, *50*, 10262-10264.
(43) Antunes, M. A.; Santos, I. C.; Bolvin, H.; Pereira, L. C. J.; Mazzanti, M.; Marcalo, J.; Almeida, M. *Dalton Trans.* **2013**, *42*, 8861-8867.
(44) MacDonald, M. R.; Fieser, M. E.; Bates, J. E.; Ziller, J. W.; Furche, F.; Evans, W. J. *J. Am. Chem. Soc.* **2013**, *135*, 13310-13313.
(45) La Pierre, H. S.; Scheurer, A.; Heinemann, F. W.; Hieringer, W.; Meyer, K. *Angew. Chem. Int. Ed.* **2014**, *53*, 7158-7162.
(46) King, D. M.; Tuna, F.; McMaster, J.; Lewis, W.; Blake, A. J.; McInnes, E. J. L.; Liddle, S. T. *Ang. Chem. Int. Ed.* **2013**, *52*, 4921-4924.
(47) Edelstein, N. M.; Lander, G. H. *The Chemistry of Actinide and Transactinide Elements*; Springer: Dordrecht, 2006; Vol. 4.
(48) Rinehart, J. D.; Bartlett, B. M.; Kozimor, S. A.; Long, J. R. *Inorg. Chim. Acta* **2008**, *361*, 3534-3538.
(49) Newell, B. S.; Schwaab, T. C.; Shores, M. P. *Inorg. Chem.* **2011**, *50*, 12108-12115.
(50) Kozimor, S. A.; Bartlett, B. M.; Rinehart, J. D.; Long, J. R. *J. Am. Chem. Soc.* **2007**, *129*, 10672-10674.
(51) Le Roy, J. J.; Gorelsky, S. I.; Korobkov, I.; Murugesu, M. *Organometallics* **2015**.
(52) Rinehart, J. D.; Fang, M.; Evans, W. J.; Long, J. R. *Nat. Chem.* **2011**, *3*, 538-542.
(53) Rinehart, J. D.; Fang, M.; Evans, W. J.; Long, J. R. *J. Am. Chem. Soc.* **2011**, *133*, 14236-14239.
(54) Moreno Pineda, E.; Chilton, N. F.; Marx, R.; Dörfel, M.; Sells, D. O.; Neugebauer, P.; Jiang, S.-D.; Collison, D.; van Slageren, J.; McInnes, E. J. L.; Winpenny, R. E. P. *Nat. Commun.* **2014**, *5*.
(55) Monteiro, B.; Roitershtein, D.; Ferreira, H.; Ascenso, J. R.; Martins, A. M.; Domingos, Â.; Marques, N. *Inorg. Chem.* **2003**, *42*, 4223-4231.
(56) Antunes, M. A.; Dias, M.; Monteiro, B.; Domingos, A.; Santos, I. C.; Marques, N. *Dalton Trans.* **2006**, 3368-3374.
(57) Antunes, M. A., Universidade de Lisboa, 2006.
(58) Camp, C.; Antunes, M. A.; Garcia, G.; Ciofini, I.; Santos, I. C.; Pecaut, J.; Almeida, M.; Marcalo, J.; Mazzanti, M. *Chem. Sci.* **2014**, *5*, 841-846.
(59) Evans, W. J.; Drummond, D. K.; Chamberlain, L. R.; Doedens, R. J.; Bott, S. G.; Zhang, H.; Atwood, J. L. *J. Am. Chem. Soc.* **1988**, *110*, 4983-4994.

(60) Takats, J.; Zhang, X. W.; Day, V. W.; Eberspacher, T. A. *Organometallics* **1993**, *12*, 4286-4288.
(61) Evans, W. J.; Forrestal, K. J.; Ziller, J. W. *J. Am. Chem. Soc.* **1998**, *120*, 9273-9282.
(62) Berg, D. J.; Boncella, J. M.; Andersen, R. A. *Organometallics* **2002**, *21*, 4622-4631.
(63) Turcitu, D.; Nief, F.; Ricard, L. *Chem. – Eur. J.* **2003**, *9*, 4916-4923.
(64) Evans, W. J.; Champagne, T. M.; Ziller, J. W. *Organometallics* **2007**, *26*, 1204-1211.
(65) Andrez, J.; Pécaut, J.; Bayle, P.-A.; Mazzanti, M. *Angew. Chem. Int. Ed.* **2014**, *53*, 10448-10452.
(66) Evans, W. J.; Drummond, D. K.; Bott, S. G.; Atwood, J. L. *Organometallics* **1986**, *5*, 2389-2391.
(67) Brady, E. D.; Clark, D. L.; Keogh, D. W.; Scott, B. L.; Watkin, J. G. *J. Am. Chem. Soc.* **2002**, *124*, 7007-7015.
(68) Evans, W. J.; Kozimor, S. A.; Ziller, J. W. *Chem. Commun.* **2005**, 4681-4683.
(69) Evans, W. J.; Miller, K. A.; Kozimor, S. A.; Ziller, J. W.; DiPasquale, A. G.; Rheingold, A. L. *Organometallics* **2007**, *26*, 3568-3576.
(70) Evans, W. J.; Montalvo, E.; Kozimor, S. A.; Miller, K. A. *J. Am. Chem. Soc.* **2008**, *130*, 12258-12259.
(71) Cladis, D. P.; Kiernicki, J. J.; Fanwick, P. E.; Bart, S. C. *Chem. Commun.* **2013**, *49*, 4169-4171.
(72) Warner, B. P.; Scott, B. L.; Burns, C. J. *Angew. Chem. Int. Ed.* **1998**, *37*, 959-960.
(73) Peters, R. G.; Warner, B. P.; Burns, C. J. *J. Am. Chem. Soc.* **1999**, *121*, 5585-5586.
(74) Diaconescu, P. L.; Arnold, P. L.; Baker, T. A.; Mindiola, D. J.; Cummins, C. C. *J. Am. Chem. Soc.* **2000**, *122*, 6108-6109.
(75) Diaconescu, P. L.; Cummins, C. C. *Inorg. Chem.* **2012**, *51*, 2902-2916.
(76) Mostad, A.; Romming, C. *Acta Chem. Scand.* **1971**, *25*, 3561-3568.
(77) Crystallographic DataBase
(78) Wietzke, R.; Mazzanti, M.; Latour, J. M.; Pecaut, J. *J. Chem. Soc., Dalton Trans.* **2000**, 4167-4173.
(79) Kindra, D. R.; Evans, W. J. *Chem. Rev.* **2014**, *114*, 8865-8882.
(80) Kraft, S. J.; Williams, U. J.; Daly, S. R.; Schelter, E. J.; Kozimor, S. A.; Boland, K. S.; Kikkawa, J. M.; Forrest, W. P.; Christensen, C. N.; Schwarz, D. E.; Fanwick, P. E.; Clark, D. L.; Conradson, S. D.; Bart, S. C. *Inorg. Chem.* **2011**, *50*, 9838-9848.
(81) Matson, E. M.; Franke, S. M.; Anderson, N. H.; Cook, T. D.; Fanwick, P. E.; Bart, S. C. *Organometallics* **2014**, *33*, 1964-1971.
(82) Lam, O. P.; Feng, P. L.; Heinemann, F. W.; O'Connor, J. M.; Meyer, K. *J. Am. Chem. Soc.* **2008**, *130*, 2806-2816.
(83) Fortier, S.; Melot, B. C.; Wu, G.; Hayton, T. W. *J. Am. Chem. Soc.* **2009**, *131*, 15512-15521.
(84) Baldovi, J. J.; Borras-Almenar, J. J.; Clemente-Juan, J. M.; Coronado, E.; Gaita-Arino, A. *Dalton Trans.* **2012**, *41*, 13705-13710.
(85) Baldoví, J. J.; Cardona-Serra, S.; Clemente-Juan, J. M.; Coronado, E.; Gaita-Ariño, A.; Palii, A. *J. Comput. Chem.* **2013**, *34*, 1961-1967.
(86) Work in preparation.
(87) Baldoví, J. J.; Clemente-Juan, J. M.; Coronado, E.; Gaita-Ariño, A. *Polyhedron* **2013**, *66*, 39-42.
(88) van Leusen, J.; Speldrich, M.; Schilder, H.; Kögerler, P. *Coord. Chem. Rev.* **2015**, *289-290*, 137-148.
(89) Speldrich, M.; Schilder, H.; Lueken, H.; Kögerler, P. *Isr. J. Chem.* **2011**, *51*, 215-227.
(90) Apostolidis, C.; Morgenstern, A.; Rebizant, J.; Kanellakopulos, B.; Walter, O.; Powietzka, B.; Karbowiak, M.; Reddmann, H.; Amberger, H. D. *Z. Anorg. Allg. Chem.* **2010**, *636*, 201-208.
(91) Cole, K. S.; Cole, R. H. *J. Chem. Phys.* **1941**, *9*, 341-351.
(92) Bruker; SMART and SAINT, Bruker AXS Inc.: Madison, Wisconsin, USA, 2004.
(93) Sheldrick, G. M.; SADABS, Bruker AXS Inc.: Madison, Wisconsin, USA, 2004.
(94) Altomare, A.; Burla, M. C.; Camalli, M.; Cascarano, G. L.; Giacovazzo, C.; Guagliardi, A.; Moliterni, A. G. G.; Polidori, G.; Spagna, R. *J. Appl. Crystallogr.* **1999**, *32*, 115-119.
(95) Sheldrick, G. M. In *SHELXL-97: Program for the Refinement of Crystal Structure*; University of Gottingen: Gottingen, Germany, 1997.
(96) Farrugia, L. J. *J. Appl. Crystallogr.* **1999**, *32*, 837-838.
(97) Macrae, C. F.; Edgington, P. R.; McCabe, P.; Pidcock, E.; Shields, G. P.; Taylor, R.; Towler, M.; van De Streek, J. *J. Appl. Crystallogr.* **2006**, *39*, 453-457.

For Table of Contents Only